Modeling Partially Unknown Dynamics with Continuous Time DMD*

Efrain Gonzalez[1] Ladan Avazpour[1] Rushikesh Kamalapurkar[2] Joel A. Rosenfeld[1]

***Abstract*— This manuscript addresses the problem of the data driven modeling of a dynamical system in the presence of partially known dynamics using an operator theoretic dynamic mode decomposition (DMD) approach. The method relies on the linearity of the Liouville operator with respect to the dynamics together with established relations between Liouville operators and occupation kernels, which embed trajectory data as a function within a reproducing kernel Hilbert space. The linearity allows for the known portion of the dynamics to be subtracted from the overall dynamics, and the Liouville operator corresponding to the unknown dynamics may thus be isolated. A model for the unknown portion of the dynamical systems may then be obtained from observed trajectory data, and this model may then be utilized for predicting future states.**

I. Introduction

Koopman based methods for dynamic mode decompositions (DMD) have proven to be effective tools for modeling unknown dynamical systems, when the system is forward complete [1]. Forward completeness is necessary for the discretization of continuous time dynamical systems, and is frequently demonstrated by showing that continuous time dynamics are globally Lipschitz continuous [3]. When the forward completeness property is satisfied, each fixed timestep, Δt yields a Koopman operator that corresponds to the discrete time dynamics obtained from the continuous time system. The collection of Koopman operators parameterized by Δt, is called the Koopman semigroup, and as $\Delta t \to 0$, the Koopman operators converge strongly to what is known as the Koopman generator, $A_f g = \nabla g(\cdot) f(\cdot)$.

Significantly, the Koopman generator is linear in the continuous dynamics (also known as the symbol of the operator). However, each Koopman operator is not linear in the dynamics. Hence, Koopman operators are a collection of operators which are nonlinear in the symbols, that approximate an operator that is linear with respect to its symbol. Moreover, Koopman generators are a proper subset of Liouville operators, where Liouville operators take the same form, but the symbols are not necessarily restricted to dynamics that are forward complete. In a series of works, the authors introduced occupation kernels, which allow for direct DMD analysis using Liouville operators that obviate the limiting process of Koopman operators [7, 6]. By removing the necessity of discretization of the dynamical systems, the occupation kernel based DMD method may be employed for systems that are not forward complete, such as $\dot{x} = 1 + x^2$. Important to the present context, this perspective allows the utilization of the linearity in the symbol of Liouville operators to take advantage of known portions of the dynamics.

In many learning contexts for dynamical systems, only a portion of the dynamics are known. For example, when an unknown second order dynamical system, $\ddot{x} = f(x)$, is converted to a first order dynamical system as $\dot{z} = \begin{pmatrix} z_2 & f(z_1) \end{pmatrix}^T$ through the augmentation of the state variable, $z = \begin{pmatrix} x & \dot{x} \end{pmatrix}^T$, the first coordinate of the dynamics are known. Another example of partially known dynamics occurs when a statefeedback controller, $u : \mathbb{R}^n \to \mathbb{R}^n$, is used in a control-affine system such as $\dot{x} = f(x) + u(x)$. However, the nonlinear nature of Koopman operators with respect to the dynamics limit the effectiveness with which this partial knowledge may be used when learning the unknown portion of the dynamics.

The linearity of the symbols for Liouville operators can be leveraged to isolate the unknown portions of the dynamics. Indeed, this property has already been effectively utilized in parameter identification in [7], where a second order system found in [4] was converted to a first order dynamical system with an augmented state variable. In this context, a collection of basis functions were pre-selected and occupation kernels in tandem with the Liouville operators corresponding to this basis were used to identify the parameters for the system, while also removing the known portions of the dynamics from consideration. Significantly, the data was leveraged to approximate the unknown dynamics without the interference of the known portions of the dynamics.

This manuscript leverages the results from [6] and [7] to provide a data driven method (i.e. without preselected basis functions) for the modeling of only the unknown portions of a dynamical system. As intimated above, this will utilize the Liouville operators' linearity with respect to their symbols, and several additional results from [7] will be exploited for computation.

II. Review of RKHSs, Occupation Kernels, and Liouville Operators

Definition 1: A reproducing kernel Hilbert space (RKHS), H over a set X is a Hilbert space of real valued functions over the set X such that for all $x \in X$ the evaluation functional, $E_x : H \to \mathbb{R}$, given as $E_x g \coloneqq g(x)$ is bounded.

Since E_x is a bounded linear functional on a Hilbert space, the Riesz representation theorem guarantees that for all $x \in$

*This research was supported by the Air Force Office of Scientific Research (AFOSR) under contract numbers FA9550-20-1-0127 and FA9550-21-1-0134, and the National Science Foundation (NSF) under award 2027976. Any opinions, findings and conclusions or recommendations expressed in this material are those of the author(s) and do not necessarily reflect the views of the sponsoring agencies.

[1]Department of Mathematics and Statistics, University of South Florida, Tampa, Fl 33620. rosenfeldj@usf.edu

[2]Department of Mechanical and Aerospace Engineering, Oklahoma State University, Stillwater, OK 74078 USA rushikesh.kamalapurkar@okstate.edu.

X there exists $k_x \in H$ such that $E_x g \coloneqq g(x) = \langle g, k_x \rangle_H$, where $\langle \cdot, \cdot \rangle_H$ is used to denote the inner product on H [5]. The kernel function corresponding to H is $K(x, y) = \langle k_y, k_x \rangle$ where k_x is referred to as the reproducing kernel centered at x. By working in the native space of the kernel function, each kernel function is associated with a feature map, $\Psi : X \to l^2(\mathbb{N})$ such that $K(x, y) = \langle \Psi(y), \Psi(x) \rangle_{l^2(\mathbb{N})}$ [8].

In [7], Liouville operators, defined below, were introduced in order to relate nonlinear dynamical systems to RKHSs.

Definition 2: Let $\dot{x} = f(x)$ be a dynamical system with the dynamics, $f : \mathbb{R}^n \to \mathbb{R}^n$, locally Lipschitz continuous, and suppose that H is a RKHS over a set X, where $X \subset \mathbb{R}^n$. The Liouville operator with symbol f, $A_f : D(A_f) \to H$, is given as

$$A_f g \coloneqq \nabla_x g \cdot f \in H, \tag{1}$$

where

$$D(A_f) \coloneqq \{g \in H : \nabla_x g \cdot f \in H\}. \tag{2}$$

The existence of densely defined Liouville operators was established in [7] and each densely defined Liouville operator is closed. Sufficient conditions were given that established when the adjoint of the Liouville operator with domain $D(A_f) \coloneqq \{g \in H : \nabla g \cdot f \in H\}$ is densely defined.

After establishing a link between RKHSs and nonlinear dynamical systems via the Liouville operator, [7] showed it was possible to establish a connection between the Liouville operator and the trajectories of a dynamical system via the occupation kernel.

Definition 3: Let $X \subset \mathbb{R}^n$, H be a RKHS of continuous functions over X, and $\gamma : [0, T] \to X$ be a continuous trajectory. The functional $g \mapsto \int_0^T g(\gamma(\tau))d\tau$ is bounded over H, and can be represented as $\langle g, \Gamma_\gamma \rangle_H = \int_0^T g(\gamma(\tau))d\tau$, for some $\Gamma_\gamma \in H$ by the Riesz representation theorem. The function Γ_γ is called the occupation kernel corresponding to γ in H.

Proposition 1: Let H be a RKHS of continuously differentiable functions over a compact set X and suppose that $f : \mathbb{R}^n \to \mathbb{R}^n$ is Lipschitz continuous corresponding to a densely defined Liouville operator. If $\gamma : [0, T] \to X$ is a trajectory as in Definition 3 that satisfies $\dot{\gamma} = f(\gamma)$, then $\Gamma_\gamma \in D(A_f^*)$, and $A_f^* \Gamma_\gamma = K(\cdot, \gamma(T)) - K(\cdot, \gamma(0))$.

It was shown in [7] that for every continuous signal, $\theta : [0, T] \to \mathbb{R}^n$, the corresponding occupation kernel, $\Gamma_\theta \in \mathcal{D}(A_f^*)$, and

$$A_f^* \Gamma_\theta(x) = \int_0^T \nabla_2 K(x, \theta(t)) f(\theta(t)) dt \tag{3}$$

where ∇_2 indicates that the gradient is performed with respect to the second variable, θ. Equation (3) will be used in the following sections in order to calculate $A_e^* \Gamma_{\gamma_i}$. Additionally, it will be important to recall that

$$\langle \Gamma_{\gamma_j}, \Gamma_{\gamma_i} \rangle = \int_0^{T_i} \int_0^{T_j} K(\gamma_i(\tau), \gamma_j(t)) dt d\tau. \tag{4}$$

III. Problem Statement

Consider the dynamical system

$$\dot{x} = h(x) + e(x) \tag{5}$$

with $h : \mathbb{R}^n \to \mathbb{R}^n$ known and $e : \mathbb{R}^n \to \mathbb{R}^n$ unknown. The objective is to determine a finite rank representation of A_e using a collection of trajectories, $\{\gamma_i : [0, T] \to \mathbb{R}^n\}_{i=1}^M$ that satisfy (5). In the sequel, the fact that $A_{h+e}^* \Gamma_{\gamma_i} = A_h^* \Gamma_{\gamma_i} + A_e^* \Gamma_{\gamma_i}$ will be pivotal in the analysis.

IV. DMD Routine for Partial Uncertainty

Suppose that $\{\gamma_i : [0, T_i] \to X\}_{i=1}^M$ is a collection of trajectories satisfying (5). The subscript in T_i indicates that every trajectory is allowed to have a different terminal time and therefore a different length. Thus, by Proposition 1, $A_{h+e}^* \Gamma_{\gamma_i} = K(\cdot, \gamma_i(T_i)) - K(\cdot, \gamma_i(0))$ for each $i = 1, \ldots, M$. Moreover, $A_h^* \Gamma_{\gamma_i}$ is computed as in (3). Consequently, for each trajectory, γ_i, corresponding to (5), the following holds

$$A_e^* \Gamma_{\gamma_i} = K(\cdot, \gamma_i(T_i)) - K(\cdot, \gamma_i(0)) - A_h^* \Gamma_{\gamma_i}. \tag{6}$$

Similar to the DMD procedure of [6], a finite rank representation of A_e^* is then determined by exploiting linearity and via the occupation kernel ordered basis, $\alpha = \{\Gamma_{\gamma_1}, \ldots, \Gamma_{\gamma_M}\}$. Let f represent the dynamics for the system and let $f = h + e$. Then from [6], $[P_\alpha A_f^*]_\alpha^\alpha = G^{-1}\mathcal{B}$ where P_α is the projection onto $\operatorname{span}(\alpha)$ and the notation $[\cdot]_\alpha^\alpha$ emphasizes that the domain and range of $P_\alpha A_f^*$ are restricted to $\operatorname{span}(\alpha)$. Recall that

$$G = \begin{bmatrix} \langle \Gamma_{\gamma_1}, \Gamma_{\gamma_1} \rangle & \cdots & \langle \Gamma_{\gamma_M}, \Gamma_{\gamma_1} \rangle \\ \vdots & \ddots & \vdots \\ \langle \Gamma_{\gamma_1}, \Gamma_{\gamma_M} \rangle & \cdots & \langle \Gamma_{\gamma_M}, \Gamma_{\gamma_M} \rangle \end{bmatrix} \tag{7}$$

and

$$\mathcal{B} = \begin{bmatrix} \langle A_f^* \Gamma_{\gamma_1}, \Gamma_{\gamma_1} \rangle & \cdots & \langle A_f^* \Gamma_{\gamma_M}, \Gamma_{\gamma_1} \rangle \\ \vdots & \ddots & \vdots \\ \langle A_f^* \Gamma_{\gamma_1}, \Gamma_{\gamma_M} \rangle & \cdots & \langle A_f^* \Gamma_{\gamma_M}, \Gamma_{\gamma_M} \rangle \end{bmatrix}. \tag{8}$$

The linearity of the Liouville operator's symbol, implies that $\mathcal{B}$ can also be written as follows:

$$\begin{bmatrix} \langle A_h^* \Gamma_{\gamma_1}, \Gamma_{\gamma_1} \rangle & \cdots & \langle A_h^* \Gamma_{\gamma_M}, \Gamma_{\gamma_1} \rangle \\ \vdots & \ddots & \vdots \\ \langle A_h^* \Gamma_{\gamma_1}, \Gamma_{\gamma_M} \rangle & \cdots & \langle A_h^* \Gamma_{\gamma_M}, \Gamma_{\gamma_M} \rangle \end{bmatrix} + \begin{bmatrix} \langle A_e^* \Gamma_{\gamma_1}, \Gamma_{\gamma_1} \rangle & \cdots & \langle A_e^* \Gamma_{\gamma_M}, \Gamma_{\gamma_1} \rangle \\ \vdots & \ddots & \vdots \\ \langle A_e^* \Gamma_{\gamma_1}, \Gamma_{\gamma_M} \rangle & \cdots & \langle A_e^* \Gamma_{\gamma_M}, \Gamma_{\gamma_M} \rangle \end{bmatrix}.$$

Therefore, after some manipulation, the following is obtained:

$$[P_\alpha A_e^*]_\alpha^\alpha = G^{-1} \left(\mathcal{B} - \begin{bmatrix} \langle A_h^* \Gamma_{\gamma_1}, \Gamma_{\gamma_1} \rangle & \cdots & \langle A_h^* \Gamma_{\gamma_M}, \Gamma_{\gamma_1} \rangle \\ \vdots & \ddots & \vdots \\ \langle A_h^* \Gamma_{\gamma_1}, \Gamma_{\gamma_M} \rangle & \cdots & \langle A_h^* \Gamma_{\gamma_M}, \Gamma_{\gamma_M} \rangle \end{bmatrix} \right) \tag{9}$$

However, the goal is to obtain a finite rank representation of $[P_\alpha A_e]_\alpha^\alpha$. Similar to the case presented above with the adjoint of the Liouville operator, the linearity of the symbols for Liouville operators implies that $[P_\alpha A_e]_\alpha^\alpha = [P_\alpha A_f]_\alpha^\alpha -$

$[P_\alpha A_h]_\alpha^\alpha$. By assuming that the occupation kernels are in the domain of the Liouville operator, it was shown in [6] that for any $q \in span(\alpha)$ and $\{\theta_j\}_{j=1}^M \subset \mathbb{R}$ a set of coefficients, it follows that

$$\langle A_f q, \Gamma_{\gamma_i}\rangle_H = \sum_{j=1}^{M} \theta_j \langle A_f \Gamma_{\gamma_j}, \Gamma_{\gamma_i}\rangle_H$$

$$= \left(\langle \Gamma_{\gamma_1}, A_f^* \Gamma_{\gamma_i}\rangle_H, \ldots, \langle \Gamma_{\gamma_M}, A_f^* \Gamma_{\gamma_i}\rangle_H\right) \begin{pmatrix} \theta_1 \\ \vdots \\ \theta_M \end{pmatrix}.$$

Proposition 1 and the properties of occupation kernels described in [7] then imply that

$$\langle \Gamma_{\gamma_j}, A_f^* \Gamma_{\gamma_i}\rangle_H = \Gamma_{\gamma_j}(\gamma_i(T)) - \Gamma_{\gamma_j}(\gamma_i(0)).$$

The above leads to the statement that $[P_\alpha A_f]_\alpha^\alpha = G^{-1}\mathcal{B}^T$.

In addition, the finite rank representation for $[P_\alpha A_h]_\alpha^\alpha$ is

$$[P_\alpha A_h]_\alpha^\alpha = G^{-1} \begin{bmatrix} \langle A_h\Gamma_{\gamma_1}, \Gamma_{\gamma_1}\rangle & \cdots & \langle A_h\Gamma_{\gamma_M}, \Gamma_{\gamma_1}\rangle \\ \vdots & \ddots & \vdots \\ \langle A_h\Gamma_{\gamma_1}, \Gamma_{\gamma_M}\rangle & \cdots & \langle A_h\Gamma_{\gamma_M}, \Gamma_{\gamma_M}\rangle \end{bmatrix}$$

The assumption that the occupation kernels are in the domain of the Liouville operator allows for the use of the definition of the Liouville operator instead of relying on its adjoint when evaluating $\langle A_h\Gamma_{\gamma_j}, \Gamma_{\gamma_i}\rangle_H$. This simplification results in

$$\langle A_h\Gamma_{\gamma_i}, \Gamma_{\gamma_j}\rangle = \int_0^{T_j}\int_0^{T_i} \nabla_1 K(\gamma_j(t), \gamma_i(\tau)) h(\gamma_j(t)) d\tau dt \tag{10}$$

Ultimately, the following finite rank representation of $[P_\alpha A_e]_\alpha^\alpha$ is obtained:

$$[P_\alpha A_e]_\alpha^\alpha = G^{-1}\left(\mathcal{B}^T - \begin{bmatrix} \langle A_h\Gamma_{\gamma_1}, \Gamma_{\gamma_1}\rangle & \cdots & \langle A_h\Gamma_{\gamma_M}, \Gamma_{\gamma_1}\rangle \\ \vdots & \ddots & \vdots \\ \langle A_h\Gamma_{\gamma_1}, \Gamma_{\gamma_M}\rangle & \cdots & \langle A_h\Gamma_{\gamma_M}, \Gamma_{\gamma_M}\rangle \end{bmatrix}\right) \tag{11}$$

In equation (10), ∇_1 indicates that the gradient is performed with respect to the first variable, γ_j.

It should be noted that the operators A_e and A_e^* are generally unbounded (cf. [7]), so with respect to convergence this is a strictly heuristic method for these operators. This is also a heuristic method for Koopman operators, which are also modally unbounded over RKHSs (e.g. [2]).

The DMD procedure aims to decompose the full state observable, $g_{id}(x) := x$, by projecting each coordinate projection function, $\pi_i(x) = x_i$, onto an eigenbasis, $\{\varphi_m\}_{m=1}^\infty$, with eigenvalues $\{\lambda_m\}_{m=1}^\infty$ of A_e. Consequently,

$$x = g_{id}(x) = \sum_{m=1}^{\infty} \xi_m \varphi_m(x).$$

The vector $\xi_m \in \mathbb{R}^n$ is called a Liouville mode, and will be referred to as a partial Liouville mode in this context.

Assuming that $[P_\alpha A_e]_\alpha^\alpha$ is diagonalizable, let $\{\nu_i\}_{i=1}^M$ be the eigenvectors for $[P_\alpha A_e]_\alpha^\alpha$ with eigenvalues $\{\lambda_i\}_{i=1}^M$. Then the functions obtained as

$$\hat{\varphi}_i(x) = \frac{1}{\sqrt{\nu_i^\dagger G \nu_i}} \begin{pmatrix} \Gamma_{\gamma_1}(x) & \cdots & \Gamma_{\gamma_M}(x) \end{pmatrix} \nu_i$$

are the normalized eigenfunctions for $[P_\alpha A_e]_\alpha^\alpha$ within the Hilbert space, and stand as a proxy for the eigenfunctions of A_e. For the basis α, $G = \left(\langle \Gamma_{\gamma_i}, \Gamma_{\gamma_j}\rangle_H\right)_{i,j=1}^M$ is the Gram matrix for the span of the occupation kernels. Furthermore,

$$V = \begin{pmatrix} \frac{\nu_1}{\sqrt{\nu_1^\dagger G \nu_1}} \cdots \frac{\nu_M}{\sqrt{\nu_M^\dagger G \nu_M}} \end{pmatrix},$$

is a matrix containing the normalized eigenvectors for $[P_\alpha A_e]_\alpha^\alpha$ and † represents the conjugate transpose.

Let

$$\hat{\xi} = \begin{pmatrix} \hat{\xi}_1 \cdots \hat{\xi}_M \end{pmatrix} = \begin{pmatrix} \int_0^{T_1} \gamma_1(t)dt \cdots \int_0^{T_M} \gamma_M(t)dt \end{pmatrix} (V^T G)^{-1}$$

be the partial Liouville modes determined by the approximation. The above notation for ξ is presented in equation (9) of [6].

Thus, a data driven model for $\dot{x}(t)$ is obtained by using the linearity of the symbols of the Liouville operator as follows:

$$\begin{aligned} \dot{x} &= \nabla g_{id}(x(t)) \left(h(x(t)) + e(x(t))\right) \\ &= A_{h+e}x(t) = A_h x(t) + A_e x(t), \end{aligned} \tag{12}$$

where the left side of the equality can be shown to be $\dot{x}(t)$ when the dynamical system is as described in equation (5) and the right side may be estimated as

$$h(x(t)) + \sum_{i=1}^{M} \lambda_i \hat{\xi}_i \hat{\varphi}_i(x(t)).$$

Therefore,

$$x(t) \approx x(0) + \int_0^t \left(h(x(\tau)) + \sum_{i=1}^{M} \lambda_i \hat{\xi}_i \hat{\varphi}_i(x(\tau))\right) d\tau. \tag{13}$$

Hence, predictions for the state variable $x(t)$ may be computed using this model obtained from the trajectory data of the dynamical system with partial unknowns.

V. Numerical Experiment

The following two subsections show the results of using the POKeDMD algorithm on two different dynamical systems: the Duffing Oscillator and the two-link robot manipulator.

A. Duffing Oscillator

In this section the developed method is applied to data generated by the Duffing oscillator which is a second order dynamical system of the form $\ddot{x} = \delta\dot{x} + \alpha x + \beta x^3 + \rho cos(wt)$. In this experiment data was simulated based on the following dynamics: $\ddot{x} = x - x^3$ which corresponds to $\delta = 0$, $\alpha = 1$, $\beta = -1$, and $\rho = 0$. Through state augmentation the second order dynamical system may be written as a first order

Algorithm 1: Pseudocode for the partial knowledge occupation kernel DMD (POKeDMD) routine of Section IV. Upon obtaining the partial Liouville modes, the normalized eigenvectors, and the eigenvalues (13) are used to compute $x(t)$.

Input: Sampled trajectories $\{\gamma_i : [0, T_i] \to \mathbb{R}^n\}_{i=1}^M$
Input: Kernel function $K : \mathbb{R}^n \times \mathbb{R}^n \to \mathbb{R}$ of an RKHS
Input: A numerical integration routine
Input: Some known dynamics for the system

Step 1 Compute the Gram matrix, G, found in (7) using a numerical integration routine and (4).
Step 2 Compute the interaction matrix, $\mathcal{B}$, found in (8) using a numerical integration routine and Proposition 1.
Step 3 Compute the matrix of $\langle A_h \Gamma_{\gamma_i}, \Gamma_{\gamma_j} \rangle$ values using (10), an integration routine, and the known dynamics for the system.
Step 4 Compute eigenvalues, λ_i, and eigenvectors, v_i, of $[P_\alpha A_e]_\alpha^\alpha$
Step 5 Compute the matrix of partial Liouville modes, ξ

Output: partial Liouville modes, ξ_i
Output: normalized eigenvectors, $\frac{v_i}{\sqrt{\nu_i^\dagger G \nu_i}}$
Output: eigenvalues λ_i for $i = 1, \ldots, M$

dynamical system, $\dot{z} = f(z)$. In the first order dynamical system created above, $z = \begin{pmatrix} z_1 & z_2 \end{pmatrix}^T = \begin{pmatrix} x & \dot{x} \end{pmatrix}^T$ and therefore $\dot{z} = \begin{pmatrix} \dot{x} & \ddot{x} \end{pmatrix}^T$. The first coordinate will be the known portion of the dynamics and is represented as $h(z) = \begin{pmatrix} z_2 & 0 \end{pmatrix}^T = \begin{pmatrix} \dot{x} & 0 \end{pmatrix}^T$, where as the second coordinate will take the place of the unknown portion of the dynamics and will be represented by $e(z) = \begin{pmatrix} 0 & \dot{z}_2 \end{pmatrix}^T = \begin{pmatrix} 0 & \ddot{x} \end{pmatrix}^T$. Therefore, the dynamical system may also be written as $\dot{z} = h(z) + e(z)$.

The initial values for each trajectory were obtained by sampling at every 0.5 interval in a grid of points that was $[-3, 3] \times [-3, 3]$. This produced 169 initial value pairs. The first number in the pair represents the initial value for the first state dimension and the second number represents the initial value for the second state dimension. The initial values, the dynamics, a time step of $h = 0.01$, and the Runge-Kutta 4 algorithm were then used to produce the 169 Duffing oscillator trajectories. Each trajectory has two state dimensions, is 99 snapshots in length, and is a signal over $[0, 1]$. Figure 1 displays the 169 trajectories created by using the above techniques. The trajectories in figure 1 will be referred to as the true trajectories.

The left most plot in figures 2, 3, and 4 displays the absolute point-wise error between the true trajectories that were created using the method described above and trajectories created using the model described in (13). The rightmost plot in each of the above mentioned figures displays the log absolute point-wise error between the true trajectories and trajectories created using the modeling technique described in [6] which is referred to here as OKDMD. The right most plots also display the log absolute point-wise error between the true trajectories and trajectories created using the POKeDMD algorithm. In this way, the right most plots are used to compare the performance of our new algorithm, POKeDMD, to its predecessor, OKDMD. The 32^{nd}, 130^{th}, and 161^{st} trajectories were randomly selected from the 169 trajectories in order to show examples of model performance over time. In these figures, the results of the POKeDMD algorithm are referred to as $\hat{x}$ whereas the results of the OKDMD algorithm are referred to as $\tilde{x}$. OKDMD is a previous method that does not use the known portion of the dynamics in order to produce a model. The exponential dot product kernel, $K(x, y) = exp\left(\frac{1}{\mu} x^T y\right)$, was used for in the POKeDMD algorithm and the OKDMD algorithm. For the POKeDMD algorithm, a kernel width of $\mu = 100$ was chosen whereas for the OKDMD algorithm a kernel width of $\mu = 50$, and a regularization value of .001 was chosen. The model created by OKDMD looks as follows:

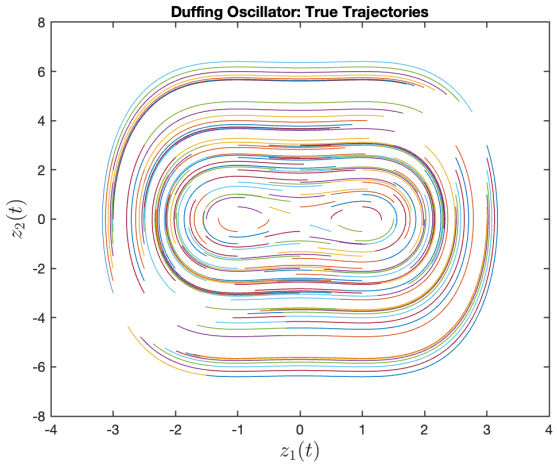

Fig. 1: This figure presents the 169 trajectories that were generated using the Duffing Oscillator dynamics, 169 initial values, a time step of $h = 0.01$, and the Runge-Kutta 4 algorithm. Each curve in this figure represents a different trajectory. Each trajectory has a different initial value.

$$\tilde{x}(t) = \sum_{i=1}^{M} \xi_i \varphi_i(x(0)) e^{\lambda_i t} \tag{14}$$

B. Two Link Robot Manipulator

In this section the developed method is applied to data generated by the dynamical system associated with the two-link robot manipulator. Let $q = (q_1\, q_2)^{\mathrm{T}} \in \mathbb{R}^2$, $\dot{q} = (\dot{q}_1\, \dot{q}_2)^{\mathrm{T}}$,

$$M(q) \coloneqq \begin{pmatrix} p_1 + 2p_3 c_2(q) & p_2 + p_3 c_2(q) \\ p_2 + p_3 c_2(q) & p_2 \end{pmatrix},$$

and

$$V_m(q, \dot{q}) = \begin{pmatrix} p_3 s_2(q)\, \dot{q}_2 & -p_3 s_2(q)\,(\dot{q}_1 + \dot{q}_2) \\ p_3 s_2(q)\, \dot{q}_1 & 0 \end{pmatrix},$$

where $p_1 = 3.473$, $p_2 = 0.196$, $p_3 = 0.242$, $c_2(q) = \cos(q_2)$, $s_2(q) = \sin(q_2)$. Also, let $E(\dot{q}) =$

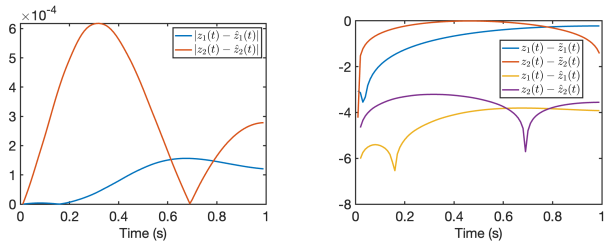

Fig. 2: The figure on the left presents the absolute point-wise error between the 32^{nd} true trajectory and the 32^{nd} trajectory generated by the POKeDMD algorithm. This figure also presents how the absolute point-wise error is progressing in time. Each curve in this figure represents a different state dimension. The figure on the right presents a comparison between the log absolute point-wise error for the 32^{nd} trajectory when using OKDMD and the log absolute error for the 32^{nd} trajectory when using POKeDMD. This figure also presents how the log absolute point-wise error is progressing in time. The OKDMD algorithm is the prior method that was used in [6] and it does not use the known portion of the dynamics in order to produce a model.

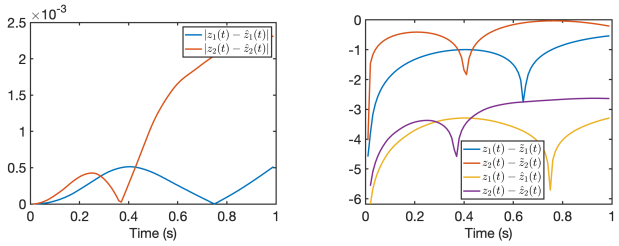

Fig. 3: The figure on the left presents the absolute point-wise error between the 130^{th} true trajectory and the 130^{th} trajectory generated by the POKeDMD algorithm. This figure also presents how the absolute point-wise error is progressing in time. Each curve in this figure represents a different state dimension. The figure on the right presents a comparison between the log absolute point-wise error for the 130^{th} trajectory when using OKDMD and the log absolute error for the 130^{th} trajectory when using POKeDMD. The figure also presents how the log absolute point-wise error is progressing in time. The OKDMD algorithm is the prior method that was used in [6] and it does not use the known portion of the dynamics in order to produce a model.

$(e_{d1}\dot{q}_1 + e_{s1}\tanh(\dot{q}_1)\ \ e_{d2}\dot{q}_2 + e_{s2}\tanh(\dot{q}_2))^{\mathrm{T}}$, where $e_{d1} = 5.3$, $e_{d2} = 1.1$, $e_{s1} = 8.45$, and $e_{s2} = 2.35$. The dynamical system for this data is of the form $\dot{x} = e(x) + g(x) \times u(x)$ where $x = \begin{pmatrix} q^{\mathrm{T}} & \dot{q}^{\mathrm{T}} \end{pmatrix}^{\mathrm{T}}$, $u(x) = Kx$, $e(x) = \begin{pmatrix} \dot{q}^{\mathrm{T}} & \left(M^{-1}(q)(-V_m(q,\dot{q})\dot{q} + E(\dot{q}))\right)^{\mathrm{T}} \end{pmatrix}$, and $g(x) = \begin{pmatrix} 0_{2\times 2} & (M^{-1}(q))^{\mathrm{T}} \end{pmatrix}^{\mathrm{T}}$, where $0_{2\times 2}$ denotes a $2x2$ matrix of zeros and $K = \begin{pmatrix} -5 & -5 \\ -15 & -15 \end{pmatrix}$.

In the above dynamical system $u(x)$ is known because it represents a feedback controller chosen by the user. Additionally, $g(x)$ is known because it represents the masses,

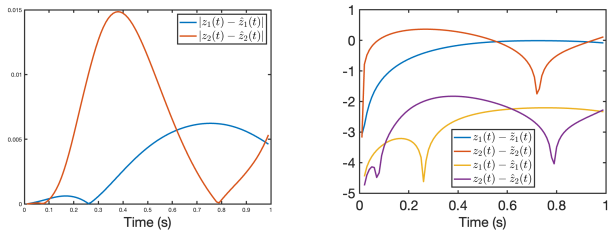

Fig. 4: The left figure presents the absolute point-wise error between the 161^{st} trajectory created by using the dynamics of the Duffing oscillator and the 161^{st} trajectory created by using the model described in (13). This figure also presents how the absolute point-wise error is progressing in time. Each curve in this figure represents a different state dimension. The figure on the right presents a comparison between the log absolute point-wise error for the 161^{st} trajectory when using OKDMD and the log absolute error for the 161^{st} trajectory when using POKeDMD. The figure also presents how the log absolute point-wise error is progressing in time. The OKDMD algorithm is the prior method that was used in [6] and it does not use the known portion of the dynamics in order to produce a model.

lengths, and moments of inertia of the robot's links.

A Halton sequence was used to generate the initial values for the 200 trajectories that were used in this experiment. The sampling was conducted over the hypercube defined by $[-1,1] \times [-1,1] \times [-1,1] \times [-1,1]$. All of the trajectories were 101 snapshots in length where the time step was set to 0.01. Each trajectory has four state dimensions, is 101 snapshots in length, and is a signal over $[0,1]$. Due to the dimensionality of this system, the trajectories for this experiment are not displayed in a plot below. However, the 32^{nd} and 161^{st} trajectories were randomly selected from the 200 true trajectories in order to show examples of model performance over time.

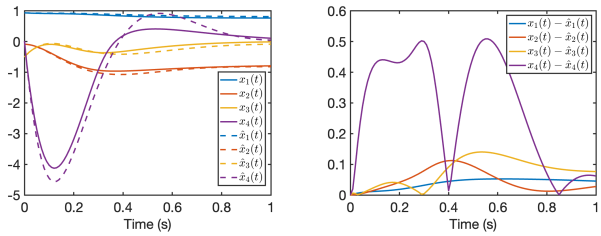

Fig. 5: The figure on the left shows the predicted and the true 32^{nd} trajectory. The predicted trajectory is shown using a dashed line and the true trajectory is displayed with a solid line. The figure on the right displays the absolute point-wise error between the true trajectories and the predicted trajectories.

The true trajectories in the left most plot of Figures 5 and 6 are represented by a solid line and were created by the above described method for simulating the data. The predicted trajectories in the left most plot of Figures 5

and 6 are represented by a dashed line and were created using the model described in (13). For the purposes of the POKeDMD algorithm the Gaussian radial basis kernel function, $K(x, y) = exp\left(\frac{-1}{\mu}\|x - y\|_2^2\right)$, with a kernel width of $\mu = 10000$ was used. Additionally, a regularization value of 0.0008 was used.

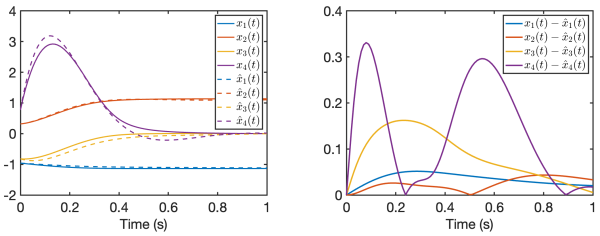

Fig. 6: The figure on the left shows the predicted and the true 161^{st} trajectory. The predicted trajectory is shown using a dashed line and the true trajectory is displayed with a solid line. The figure on the right displays the absolute point-wise error between the true trajectories and the predicted trajectories.

The right most plots of Figures 5 and 6 display the absolute point-wise error between the true trajectories and the predicted trajectories.

VI. Discussion

In the Duffing Oscillator example, the POKeDMD method isolates $h(z)$ from the rest of the dynamics, which are considered unknown. This methodology is uniquely suited to Liouville operators and occupation kernels because the Liouville operator is linear with respect to the dynamics. This linearity property is not present in Koopman based methods. Importantly, through the removal of the known portion of the dynamics, accurate reconstruction is made feasible, where previous iterations of Liouville based DMD methods have struggled to maintain accurate reconstruction of trajectories stemming from this dynamical system. By checking the absolute point-wise error between the trajectories generated for the numerical experiment and the trajectories created using the model described in (13), it is possible to see that the model is adequately approximating the unknown dynamics of the Duffing Oscillator. It is easiest to see the truth in the above statement by looking over figures 2, 3, and 4. Furthermore, it can be said that leveraging known dynamics in the way done by the POKeDMD algorithm produces a better model than would otherwise be created by OKDMD. For evidence of the above, the reader should again turn to the aforementioned figures in which it can be seen that the log absolute point-wise error is much greater in the case of the previous algorithm (OKDMD) as opposed to the error for the new algorithm (POKeDMD). In figures 2, 3, and 4 it is evident that the absolute point-wise error is increasing over time. This behavior is to be expected because by using numerical methods to approximate the solution to the initial value problem, one introduces an error that accumulates over time.

Figures 5 and 6 serve as an additional example of the effectiveness of the POKeDMD algorithm on a control-affine system with a statefeedback controller. The experiments conducted on the two link robot manipulator further highlight the way in which the developed algorithm may be used by the control community. Using limited knowledge about the system the POKeDMD algorithm is able to construct a model that performs well when evaluating the absolute point-wise error between the model predictions and the true trajectories.

VII. Conclusion

Liouville operators have been presented as a way to model continuous time dynamical systems without discretization and methods that use Liouville operators have been shown to be more flexible in learning contexts for dynamical systems than their Koopman generator counterparts [7]. This paper expanded on the usefulness of applying Liouville operators to continuous time dynamical systems by leveraging the linearity of the Liouville operators with respect to their symbols. This allowed for the isolation of the unknown portion of the dynamics and more efficiently leveraged the data to learn only this unknown portion of the dynamics. The theoretical framework established in this paper is further bolstered by the results obtained from the numerical experiments, which highlight the capabilities of this method.

References

[1] A. Bittracher, P. Koltai, and O. Junge. "Pseudogenerators of spatial transfer operators". In: *SIAM Journal on Applied Dynamical Systems* 14.3 (2015), pp. 1478–1517.

[2] B. Carswell, B. D. MacCluer, and A. Schuster. "Composition operators on the Fock space". In: *Acta Sci. Math.(Szeged)* 69.3-4 (2003), pp. 871–887.

[3] E. A. Coddington and N. Levinson. *Theory of ordinary differential equations*. Tata McGraw-Hill Education, 1955.

[4] A. Janot, M. Gautier, and M. Brunot. "Data set and reference models of EMPS". In: *Nonlinear System Identification Benchmarks*. 2019.

[5] V. I. Paulsen and M. Raghupathi. *An introduction to the theory of reproducing kernel Hilbert spaces*. Vol. 152. Cambridge Studies in Advanced Mathematics. Cambridge University Press, Cambridge, 2016, pp. x+182. ISBN: 978-1-107-10409-9. DOI: 10.1017/CBO9781316219232. URL: https://doi.org/10.1017/CBO9781316219232.

[6] J. A. Rosenfeld et al. "Dynamic mode decomposition for continuous time systems with the Liouville operator". In: *Journal of Nonlinear Science* 32.1 (2022), pp. 1–30.

[7] J. A. Rosenfeld et al. *The Occupation Kernel Method for Nonlinear System Identification*. 2019. arXiv: 1909.11792 [math.OC].

[8] Ingo Steinwart and Andreas Christmann. *Support vector machines*. Springer Science & Business Media, 2008.